

# A combined approach for the enhancement and segmentation of mammograms using modified fuzzy C-means method in wavelet domain

Subodh Srivastava, Neeraj Sharma, S. K. Singh<sup>1</sup>, R. Srivastava<sup>1</sup>

School of Bio-Medical Engineering, <sup>1</sup>Department of Computer Science and Engineering, Indian Institute of Technology, Banaras Hindu University, Varanasi, Uttar Pradesh, India

Received on: 28.12.2013    Review completed on: 16.05.2014    Accepted on: 17.05.2014

## ABSTRACT

In this paper, a combined approach for enhancement and segmentation of mammograms is proposed. In preprocessing stage, a contrast limited adaptive histogram equalization (CLAHE) method is applied to obtain the better contrast mammograms. After this, the proposed combined methods are applied. In the first step of the proposed approach, a two dimensional (2D) discrete wavelet transform (DWT) is applied to all the input images. In the second step, a proposed nonlinear complex diffusion based unsharp masking and crispening method is applied on the approximation coefficients of the wavelet transformed images to further highlight the abnormalities such as micro-calcifications, tumours, etc., to reduce the false positives (FPs). Thirdly, a modified fuzzy c-means (FCM) segmentation method is applied on the output of the second step. In the modified FCM method, the mutual information is proposed as a similarity measure in place of conventional Euclidian distance based dissimilarity measure for FCM segmentation. Finally, the inverse 2D-DWT is applied. The efficacy of the proposed unsharp masking and crispening method for image enhancement is evaluated in terms of signal-to-noise ratio (SNR) and that of the proposed segmentation method is evaluated in terms of random index (RI), global consistency error (GCE), and variation of information (Vol). The performance of the proposed segmentation approach is compared with the other commonly used segmentation approaches such as Otsu's thresholding, texture based, k-means, and FCM clustering as well as thresholding. From the obtained results, it is observed that the proposed segmentation approach performs better and takes lesser processing time in comparison to the standard FCM and other segmentation methods in consideration.

**Key words:** Mammogram segmentation; mammogram enhancement; modified fuzzy c-means segmentation; mutual information; performance evaluation; wavelet based segmentation

## Introduction

According to American Cancer Society's, the Cancer facts and Figures 2013,<sup>[1]</sup> breast cancer is the most common cancer among women, except for skin cancers. About 1 in 8 (12%) women in the US will develop invasive breast cancer

during their lifetime. The American Cancer Society for breast cancer in the United States for 2013 estimates that about 232,340 new cases of invasive breast cancer will be diagnosed in women, about 64,640 new cases of carcinoma *in situ* (CIS) will be diagnosed (CIS is non-invasive and is the earliest form of breast cancer), and about 39,620 women will die from breast cancer. Women in the India have about a 1 in 9 lifetime risk of developing invasive breast cancer. The early detection and diagnosis of breast cancer can increase the survival rate and effective treatment options in time. In screening mammography, radiographic imaging of the breast is currently the most effective and cheap tool for early detection of breast cancer. In screening mammogram program, the digital mammographic images are obtained and collected for the suspicious cases and the radiologists visually examine the mammograms for specific abnormalities. Breast image analysis can be performed using many imaging modalities such as digital mammography, magnetic resonance imaging (MRI), nuclear imaging and ultrasound. But the digital mammography is more popular and commonly used imaging tool for breast cancer detection due to its cost effectiveness as well as its higher ability

## Address for correspondence:

Dr. Subodh Srivastava,  
Ph.D., School of Bio-Medical Engineering, Indian Institute of Technology, Banaras Hindu University,  
Varanasi - 221 005, Uttar Pradesh, India.  
E-mail: subodhresonance@gmail.com

Access this article online	
Quick Response Code:	Website: <a href="http://www.jmp.org.in">www.jmp.org.in</a>
	DOI: 10.4103/0971-6203.139007

to detect the disease. Mammography is low dose X-ray procedure that allows visualisation of internal structure of the breast. The most common breast abnormalities that may indicate breast cancer include masses, calcifications, architectural distortion, and bilateral symmetry. The breast lesions have a wide range of features that can indicate malignant changes, but can also be part of benign changes. They are sometimes indistinguishable from the surrounding tissue which makes the detection and diagnosis of breast cancer more difficult. Knowing the limitations of human observers and its difficulty for radiologists to provide both accurate and uniform evaluation for the enormous number of mammograms generated in widespread screening, automation of the breast cancer detection and diagnosis through a software CAD tool may help in accurate and uniform detection and diagnosis of breast cancer. Computer aided detection (CADe) and diagnosis (CADx), combined called as CAD, is used to help radiologists in interpretation of mammograms and is usually used as a second opinion by the radiologists. Improving CAD performance increases the treatment options and a cure is more likely. Also, to help the radiologists in screening large number of mammograms, the use of a CAD tool maybe helpful in exact prognosis free from human error analysis.

The major steps involved in the design and analysis of an automated CAD tool for cancer detection from mammograms include: Preprocessing (restoration and enhancement), image segmentation, feature extraction, feature selection and classification. The design and analysis of efficient algorithms for each step play an important role in deciding the efficacy and correctness of the overall CAD tool. Image enhancement and segmentation plays an important role in the design and development for the said CAD tool. In image segmentation the basic aim is to separate the suspicious region, that may contain abnormalities in mammograms such as micro-calcifications, tumors etc., from the background tissue. The segmentation process partitions the mammogram into several non-overlapping regions, extract regions of interests (ROIs), and locate the suspicious areas, such as micro-calcifications and tumours which are candidates for ROIs. The suspicious area is an area that is brighter than its surroundings, has almost uniform density, has a regular shape with varying size, and has fuzzy boundaries.<sup>[2]</sup> A better image enhancement technique, applied prior to segmentation process, for highlighting and enhancing the abnormalities in mammograms may further reduce the false positives (FPs) during cancer detection. Hence, image segmentation is a very essential and important step that determines the sensitivity of the overall CAD tool. The results for segmentation is supposed to include the regions containing all abnormalities even with some FPs, if left out, which can be removed at a later stage of the algorithms for CAD tool design. An overview of enhancement and segmentation techniques for mammograms is given as below.

### **Overview of enhancement techniques for mammograms**

The various methods<sup>[3-6]</sup> which exists in literature for the enhancement of mammograms may be broadly divided into three categories which include global approaches,<sup>[7-10]</sup> local approaches,<sup>[11-15]</sup> and multiscale processing based approaches.<sup>[16-20]</sup> The global approach based methods reassign the intensity values of pixels to make the new distribution of the intensities uniform to the maximum extent. This method is effective in enhancing the entire image with low contrast. The main disadvantages of global schemes are that they cannot enhance the textual information and working only for the images having one object. The local approaches for image enhancement are feature-based or use nonlinear mapping locally. These methods are effective in local texture enhancement. The main disadvantages of the local schemes are that they cannot enhance the entire image very well. The multiscale processing based enhancement techniques are based on wavelet transformation and they are flexible to select local features to be enhanced and able to suppress the noise. If the mother wavelet and weight modification functions are chosen carefully, the wavelet based method can perform very well.<sup>[16]</sup> Some of the commonly used methods available in literature for the enhancement of mammograms include contrast limited histogram equalization (CLAHE) based technique,<sup>[11]</sup> density-weighted contrast enhancement (DWCE),<sup>[21]</sup> logic filters,<sup>[9,22,23]</sup> iris filters<sup>[24,25]</sup> and difference of Gaussians (DoG).<sup>[26]</sup> The DWCE is used in two stages, at first it is applied globally to isolate the suspected area, then it is used locally to refine the segmentation. It works in conjunction with Laplacian of Gaussian (LoG) filter. The logic filter is a nonlinear filter, and logic operators AND, OR, and XOR are used. The concrete logic expressions depend on the prior information, and the filter structure influences the results. Iris filter is an adaptive filter and it is applied locally. The Gaussian filter ROIs are highlighted by a DOG filter and it can reduce number of FPs during segmentation process.

Here, in this paper, in addition to image enhancement we propose to incorporate an unsharp masking and crispening operator to further highlight and sharpen the abnormalities using a nonlinear complex diffusion based approach.

### **Overview of segmentation techniques for mammograms**

In literature,<sup>[28,29,31,32]</sup> supervised and unsupervised are two types of image segmentation approaches. The supervised segmentation or model based method use the prior knowledge about the object and background regions to be segmented. The prior information is used to determine if specific regions are present within an image or not. The unsupervised segmentation partitions an image into a set of regions which are distinct and uniform with respect to specific properties, such as grey-level, texture or color. The

classical approaches for solving unsupervised segmentation are divided in three major groups namely region-based methods, which divide the image into homogeneous and spatially connected regions; contour-based methods, which depends on the boundaries of regions; and clustering methods, which group together those pixels having the same properties and might result in non-connected regions. According to their natures, there are four broad categories of image segmentation approaches in literature<sup>[3]</sup> for the segmentation of mammograms which include classical techniques, fuzzy techniques, bilateral image subtraction, rough set based approaches<sup>[57-60]</sup> and multiscale techniques. A brief review of various segmentation approaches may be found in paper.<sup>[3]</sup>

In this paper, a modified fuzzy c-means (FCM) segmentation method based on mutual information in wavelet domain is proposed for segmenting the abnormalities in mammograms. Before applying the proposed segmentation approach, a PDE based unsharp masking and crispening method is proposed and applied on the mammograms to highlight the details of the abnormalities such as micro-calcifications etc., to reduce the false positives (FPs) during segmentation process.

The proposed segmentation method is compared with the Otsu's optimal thresholding,<sup>[34-35,37]</sup> texture based segmentation method,<sup>[36]</sup> k-means segmentation,<sup>[31]</sup> and FCM based thresholding<sup>[3,37]</sup> based segmentation method.

Reasons for using fuzzy technique based image segmentation algorithm<sup>[3,37]</sup> are as follows: Since the contrast in mammograms is very low and the boundary between normal tissue and tumours is unclear, the traditional segmentation methods might not work well. The classical region growing based segmentation technique tries to precisely define ROIs, but to find a criterion for segmentation is difficult as most of the malignant tumors with fuzzy boundaries extend from a dense core region to the surrounding tissues. Similarly, the classical global or local thresholding techniques<sup>[3]</sup> try to segment ROIs, but the techniques are only effective for the objects with clear boundaries. The fuzzy logic based approaches are useful for segmenting suspicious regions<sup>[3,32]</sup> and are capable of addressing above issues.

The categorization and summary of various commonly used mammogram segmentation methods are presented in [Table 1].

**Table 1: Categorization and summary of segmentation methods**

<i>Broad segmentation approaches</i>	<i>Sub-categories of segmentation approaches</i>	<i>Brief description of methods</i>	<i>Advantages and disadvantages</i>
1. Classical approaches	1.1 Global thresholding	Global thresholding methods use global information such as histogram of the image/gray level intensity values for the segmentation process Multiple thresholding can be used for segmenting multiple objects	This method is easy to implement and widely used but not well for finding ROIs. False positives and false negatives may be very high
	1.2 Local thresholding	Local thresholding uses gray level intensity values and local statistics of images for segmentation If in addition to the above information the coordinates of the pixels are also used to determine the threshold value for segmentation, it is called adaptive or dynamic thresholding	Local thresholding is more precise than global method and is better for mass detection. It can't accurately separate the pixels in suitable sets. Hence, used as initialization for global thresholding Adaptive thresholding is computationally expensive and not suitable for real time applications
	1.3 Optimal thresholding Example: Otsu's global thresholding	This algorithm proceeds automatically, is unsupervised, and use within-class variance and between-class variance to select an optimal threshold for segmentation	If threshold values are optimal, then it may provide the good results and widely used. However, may not be good for finding ROIs and FPs may be high. It assumes that two group of pixels overlap. If only one combined histogram is available then finding the optimal threshold value becomes a difficult task
	1.4 Based on pixel relationships		
	1.4.1 Markov random field or Gibbs random field Example: Simulated annealing	To represent the global relationship this method uses the local neighbourhood relationship This method starts with a random seed pixel, grows iteratively and aggregate pixels having similar properties	Produce better segmentation results but require complex statistical computations and takes large processing time The segmentation result depends on the selection of the seed point and it is sensitive to noises
1.4.2 Region growing Examples: Simple graphical seed fill, Adaptive thresholding, Adaptive region growing etc.			

*Contd...*

**Table 1: Continued**

<i>Broad segmentation approaches</i>	<i>Sub-categories of segmentation approaches</i>	<i>Brief description of methods</i>	<i>Advantages and disadvantages</i>
	1.4.3 Region clustering Example: K-means	It finds the region of interest directly without any prior information .i.e. it finds the clusters/ROIs based on some similarity measures e.g., Euclidian distance	This method is similar to the region growing method and does not use local spatial statistics of the pixels. It assumes the pixels of a cluster have constant intensity. The numbers of clusters have to be specified initially
	1.5 Edge detection Examples: Density-weighted contrast enhancement, Logic filters, Iris filters, Difference of Gaussians, and Contour based methods	Here, segmentation is based on edge detection based on discontinuity calculation using first and second order derivatives of the image pixels	This method may reduce number of false positives. Performance may depend on initialization such as in contour based methods
	1.6 Template matching	Segmentation of the object such as masses is obtained from background using available prototypes	It is easy to implement and may provide good results if prototypes are appropriate It depends on the prior information of masses for prototypes and may result in large false positives. Suitable only for mass detection
	1.7 Stochastic relaxation	It is unsupervised and evidential constrained optimization method based segmentation method	It is based on a statistical model and builds optimal label maps to separate tissue and suspicious areas. It takes large processing time and involves complex parameter estimation
	1.8 Texture based segmentation (Entropy filter based segmentation)	Performs segmentation based on texture information	Suitable for texture segmentation. May not provide good results for mammograms
2. Fuzzy Techniques	2.1 Fuzzy region clustering or growing 2.2 Fuzzy thresholding	It uses fuzzy operators, properties and inference rules to deal with uncertainty in images	It can handle the unclear boundaries between normal and suspicious tissues in mammograms but requires effort in designing suitable membership functions and rules
3. Bilateral Image subtraction		This segmentation method is based on the normal symmetry between the left and right breasts. The differences between the left and right mammograms give the suspicious region	It is easy to implement but difficult to register the left and right breast correctly
4. Rough Set based image segmentation <sup>[59]</sup>		The basic idea behind segmentation-based rough sets is that while some cases may be clearly labeled as being in a set A called the positive region in rough sets theory, and some cases may be clearly labeled as not being in set A called the negative region, limited information prevent from labeling all possible cases clearly. The remaining cases cannot be distinguished and lie in what is known as the boundary region	Rough sets treat nominal data based on concepts of categorization and approximation for image segmentation. This approach may also provide better results
5. Multi-scale technique	Wavelet based segmentation	It uses discrete wavelet transform for further processing	It is capable of discriminating different frequencies/scales and easily detects transients. It can preserve the resolution of the portion of ROI and it does not need any prior information. Selecting suitable mother wavelets and weight modifying functions requires some effort

FPs: False positives, DWCE: Density-weighted contrast enhancement, ROI: Region of interest, FNs: False negatives, MRF: Markov random field, GRF: Gibbs random field

The organization of the paper is as follows: Section 1 of the paper presents the brief introduction of the problem; Section 2 of the paper presents the methods and models, that is the proposed method in detail along with the justification for the proposed models; Section 3 of the paper presents the results, performance analysis, and discussions; Section 4 of the paper presents the conclusions of the work.

## Materials and Methods

In this paper, an image enhancement and segmentation technique is proposed for the segmentation of mammograms for breast cancer detection. The proposed method consists of following steps as illustrated in [Figure 1].

**Algorithm for the proposed method**

Step 1: In the first step, CLAHE based enhancement technique is applied on original low contrast mammogram to enhance them in to good contrast images.

Step 2: Two levels of 2D discrete wavelet transform (DWT) is applied on the output obtained in the first step. This step is applied to perform the segmentation at various scales (multi-resolution) and also the wavelets can detect more easily the transient signals or abrupt changes caused by various gray level changes in images due to micro-calcifications and other abnormalities.

The other advantage being the faster processing of FCM based clustering method used in segmentation step.

Step 3: In this step, the proposed nonlinear complex diffusion based unsharp masking and crispening method is applied on the enhanced mammogram

to further enhance and highlight the abnormalities and fine details present in mammograms such as micro-calcifications and tumors. This step help the segmentation process in producing the good results and increase the cancer detection rate by the CAD tool by reducing the false positives.

Step 4: The proposed modified FCM thresholding based image segmentation is applied on mammograms obtained in step 3.

Step 5: Inverse wavelet transform is applied to reconstruct the final segmented image in spatial domain.

In step 2 of the algorithm, it had been practically examined that two levels of DWT based segmentation is providing better results and very close to that of third level of DWT decomposition. Three levels of DWT decomposition may also be used but for large scale processing of mammograms computational complexity may increase.

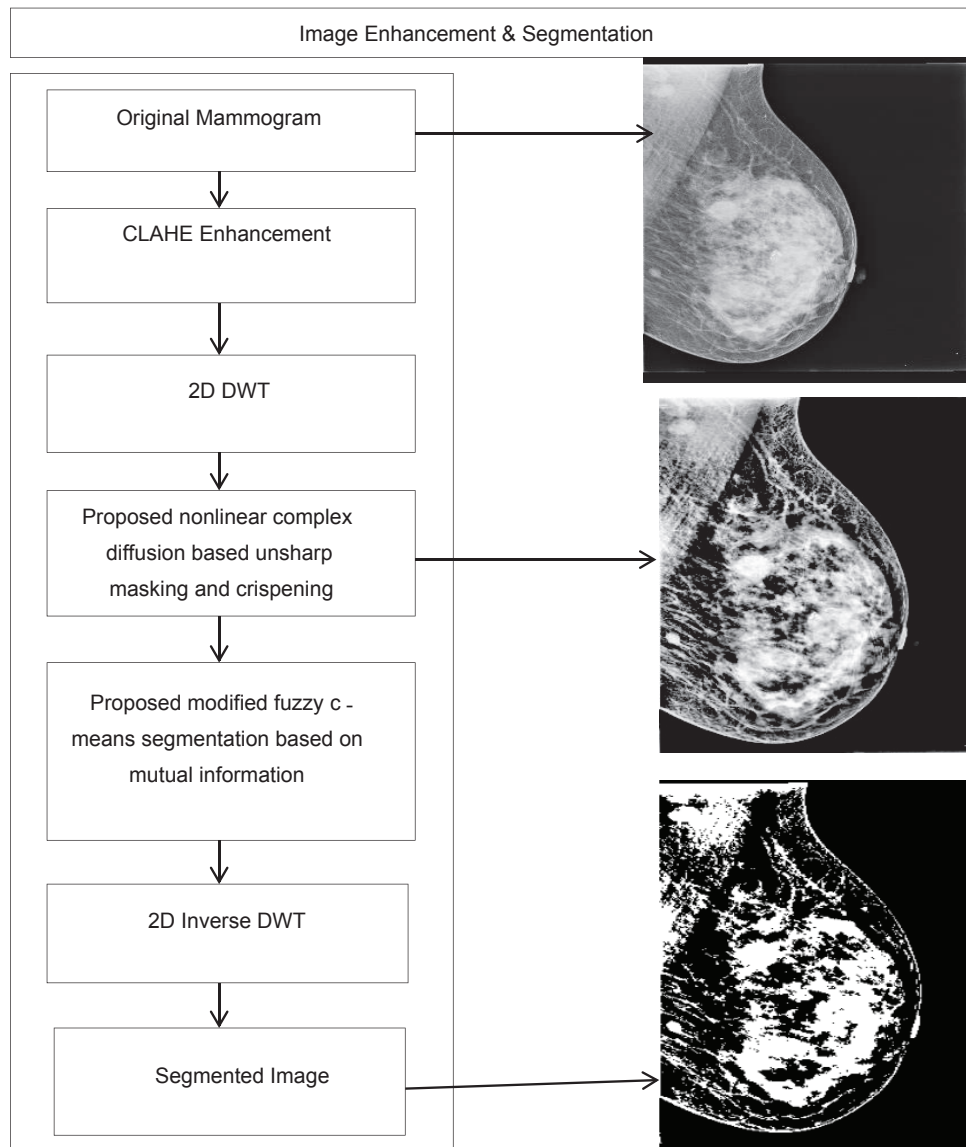


Figure 1: Proposed image enhancement and segmentation framework

The proposed steps 3 and 4 of the algorithms are described as follows:

### **Nonlinear complex diffusion based approach for unsharp masking and crispening of mammograms**

The basic procedure<sup>[27,39]</sup> for unsharp masking and crispening the image is as follows: In the first step, a low-pass filter is applied on the original image for smoothening the same. In the second step, the edge description and other desired high frequency components of an image are calculated by subtracting the smoothened image obtained in the first step from the original image. In the third and last step, the edge image obtained in second step is used for sharpening the edges and other high variation components of original image by adding back it to the original signal. The unsharp masking produces an edge image  $I_e(x, y)$  from an input image  $I(x, y)$  via

$$I_e(x, y) = I(x, y) - I_{smooth}(x, y) \quad (1)$$

where  $I_{smooth}(x, y)$  is the smoothened version of  $I(x, y)$ .

The complete unsharp masking operator reads

$$I_{sharp}(x, y) = I(x, y) + k * I_e(x, y) \quad (2)$$

where  $k$  is a scaling constant,  $k > 0$ . The reasonable values for  $k$  varies between 0.2-0.8, with the larger values providing increasing amount of sharpening.

A commonly used gradient function for smoothening the image. that is  $I_{smooth}(x, y)$  and the unsharp masks for producing an edge image is negative discrete Laplacian filter which is a second order derivative of an image taken in both  $x$  and  $y$  directions.

$$I_{smooth}(x, y) = \nabla^2 I(x, y) = [I(x-1, y) + I(x, y-1) + I(x+1, y) + I(x, y+1) - 4I(x, y)] \quad (3)$$

After substituting Eq. (3) in Eq. (1), the Eq. (1) reads

$$I_e(x, y) = I(x, y) - I_{smooth}(x, y) = I(x, y) - \nabla^2 I(x, y) \quad (4)$$

Another method used in place of discrete Laplacian is Laplacian of Gaussian (LoG). In this case since the kernel peak is positive, the edge image is subtracted, rather than added back to the original image. The disadvantages of these schemes are that gradient images produced by both filters, Laplacian and LoG, produces the side effects of ringing or introduction of additional intensity image structure and this ringing occurs at high contrast edges. Hence, the unsharp filter is a powerful sharpening operator, but it also produces a poor result in the presence of noise.

In Eq. (4), the second term of RHS is Laplacian which is used as unsharp mask to produce the edge image defined as,  $I_{smooth}(x, y) = I(x, y)$  is a Heat equation which performs the isotropic diffusion to de-noise the image. The smoothing process can be regarded as an evolution process governed by a PDE that performs regularization of the image<sup>[40]</sup> as follows.

$$\frac{\partial I}{\partial t} = \nabla^2 I(x, y) \quad (5)$$

To effectively remove the noise from the image and preserving as well as enhancing the edge structure of an image, the Eq. (5) can be modified according to Perona and Malik<sup>[40]</sup> which achieves both noise removal and edge enhancement through the use of a non-uniform diffusion which acts as non-uniform inverse diffusion near edges<sup>[40]</sup> and as linear heat equation like diffusion in homogeneous regions without edges. The basic idea is that heat Eq. (5) for linear diffusion can be written in divergence form:

$$\frac{\partial I}{\partial t} = \nabla \cdot \nabla I = \nabla \cdot \nabla I \quad (6)$$

The introduction of a conductivity coefficient  $c$  in Eq. (6) makes it possible to make the diffusion adaptive to local image structure:<sup>[41]</sup>

$$\frac{\partial I}{\partial t} = \nabla \cdot \nabla I \quad (7)$$

where the function  $c = c(I, I_x, I_{xx}, \dots)$  is a function of local image differential structure that depends on local partial derivatives.

The above anisotropic diffusion based process involves the properties of forward diffusion on real axis which is more useful for analysing real valued grey images but may not be useful for reducing those noises which are near to threshold values and may produce staircase and ringing effects. Hence, to overcome these issues, in this paper, a nonlinear complex diffusion based filter as defined in<sup>[41]</sup> is used. In complex diffusion based processes, the imaginary part serve as an edge detector, smoothed second derivative scaled by time, when the complex diffusion coefficient approaches the real axis. The complex diffusion based processes do not produce blocky artefacts or stair casing effects during the evolution process of the image. It also preserves the edges and fine structures within the image and results do not change by changing illumination conditions. These properties are helpful in mammographic image analysis for better diagnosis. The nonlinear complex diffusion based filter reads<sup>[41]</sup>:

$$\frac{\partial I}{\partial t} = \nabla \cdot \{c[\text{Im}(I)]\nabla I\} \quad (8a)$$

$$\text{with initial condition } I_{t=0} = I_0 \quad (8b)$$

The diffusion coefficient  $c[\text{Im}(I)]$  used in Equation 8(a) is defined as follows<sup>[41]</sup>:

$$c[\text{Im}(I)] = \frac{e^{i\theta}}{1 + \left(\frac{\text{Im}(I)}{k\theta}\right)^2}$$

In above equation,  $\text{Im}(I)$  is the imaginary part of the image, and  $k$  is an edge threshold parameter which ranges from 1-1.5.<sup>[41]</sup> A qualitative property of edge detection, that is the second smoothed derivative is described by the imaginary part of the image for small value of  $\theta$ , whereas real values depict the properties of ordinary Gaussian scale-space. For large values of  $\theta$ , the imaginary part feeds back in to the real part creating the wave-like ringing effect which is an undesirable property. Here, for experimentation purposes value of  $\theta$  is chosen to be  $\pi/30$ .

Further, the Eq. (8a) can be written as

$$\frac{\partial I}{\partial t} = \frac{I_{\text{smooth}}(x,y) - I(x,y)}{\Delta t} = \nabla \bullet \{c[\text{Im}(I)]\nabla I\}$$

$$I_{\text{smooth}}(x,y) = I(x,y) + \Delta t \{D[c \text{Im}(I) DI]\} \quad (9)$$

where  $\Delta t = 0-0.25$  for stability purposes.

The R.H.S. of Eq. (9) can be discretized using forward time central difference scheme (FTCS).<sup>[42]</sup> The algorithm for unsharp masking and crispening of digital mammograms is as follows:

**Algorithm–Nonlinear complex diffusion based unsharp masking and crispening of mammograms**

1. The input image  $I(x,y)$  is the original mammogram which may be noisy.
2. Perform the smoothening of the image using equation (9).

$$I_{\text{smooth}}(x,y) = I(x,y) + \lambda t \{D[c \text{Im}(I) DI]\}$$

3. Obtain the edge description of the image according to equation (1)

$$I_e(x,y) = I(x,y) - I_{\text{smooth}}(x,y)$$

4. Finally, perform the unsharp masking and crispening step as follows:

$$I_{\text{sharp}}(x,y) = I(x,y) + k^* I_e(x,y).$$

The last step (4) is used to obtain the sharpened with crisped edges and  $k$  is a scaling constant,  $k > 0$ . The reasonable values for  $k$  varies between 0.2-0.8, with the larger values providing increasing amount of sharpening.

**Proposed modified fuzzy c-means thresholding based image segmentation using mutual information**

The working of the FCM clustering approach is given as follows:<sup>[37,38,60]</sup>

In fuzzy approach based partitioning, the Gaussian membership matrix  $(U) = [u_{ij}]$  is randomly initialized according to Eq. (10), where  $u_{ij}$  being the degree of membership function of the data point of  $i^{\text{th}}$  cluster  $x_i$ . The membership matrix  $U$  is allowed to have elements with values between 0 and 1 but the summation of degrees of belongingness of a data point to all clusters or partitions is always equal to unity:

$$\sum_{i=1}^c u_{ij} = 1, \forall j = 1..n \quad (10)$$

The performance index (PI) or cost function for membership matrix  $U$  and  $c_i$  used in FCM is given by Eq.(11) which reads

$$J(U, c_1, c_2, \dots, c_n) = \sum_{i=1}^c J_i = \sum_{i=1}^c \sum_{j=1}^n u_{ij}^m d_{ij}^2 \quad (11)$$

where  $u_{ij}$  is between 0 and 1,  $c_i$  is the centroid of the fuzzy cluster  $i$ ,  $d_{ij} = \|c_i - x_j\|$  is the Euclidian distance between  $i^{\text{th}}$  centroid ( $c_i$ ) of the cluster and  $j^{\text{th}}$  data point, and  $m \in [1, \infty)$  is a weighting exponent. To form a partition of similar pixels having nearly equal gray level intensities the Euclidian distance measure is computed and two pixels having minimum of the distance are placed in same cluster or partition. To reach a minimum of dissimilarity function or to find the minimum cost function given by Eq. (11), the following two conditions, given by Eqs. (12) and (13), must be satisfied.

$$c_i = \frac{\sum_{j=1}^n U_{ij}^m x_j}{\sum_{j=1}^n U_{ij}^m} \quad (12)$$

$$U_{ij} = \frac{1}{\sum_{k=1}^c \left(\frac{d_{ij}}{d_{kj}}\right)^{2/(m-1)}} \quad (13)$$

The FCM algorithm works iteratively through the above two conditions until there is no more improvement.

The limitations of the standard FCM based segmentation algorithms are as follows:

The main requirement of this algorithm is that the number of clusters should be known apriori. The performance of FCM depends on the initial membership matrix values hence the algorithm is run for several times, each starting with different values of membership grades of data points. Although the original intensity-based FCM algorithm functions well on segmenting most noise-free images, it fails to segment images corrupted by noise, outliers, and other imaging artifacts, such as the intensity inhomogeneity induced by the various abnormalities such as micro-calcifications in mammograms, and thus leads to its non-robust results mainly due to the use of (a) Non-robust Euclidean distance and (b) disregard of spatial contextual information in image.<sup>[43]</sup> Hence, FCM

lacks enough robustness to noise and outliers and is not suitable for revealing non-Euclidean structure of the input data due to the use of Euclidean distance (L2 norm). To deal with this problem, some researchers adopted robust distance measures such as  $L_p$  norms ( $0 < p \leq 1$ )<sup>[44-46]</sup> to replace the L2 norm in the FCM objective function for reducing the effect of outliers on clustering results, and while many other algorithms have also been proposed to deal with the second problem by incorporating spatial information into original FCM objective function.<sup>[47-50]</sup>

Hence, to deal with above issues, in this paper, a mutual information based distance measure available in<sup>[30]</sup> is used for FCM. The other advantage of using mutual information as distance measure is that it can capture any correlative behaviour (positive, negative, and nonlinear) between image pixel values whereas the Euclidean distance measure can capture only positive correlations between pixel patterns.

Therefore, the Euclidian distance measure, used in classical FCM segmentation as a distance function for dissimilarity measurement to from the clusters of similar pixels, is replaced by the distance measure defined in terms of mutual information due to the reasons discussed as above. In this paper, the idea for the gene clustering based on cluster wide mutual Information used in paper<sup>[30]</sup> is adopted to define the distance measure used by FCM for the segmentation of mammograms.

For discrete variables, the mutual information  $I$  of two variables  $X$  and  $Y$  is defined as measure of information about  $X$  (or  $Y$ ) contained in  $Y$  (or  $X$ )<sup>[30]</sup>:

$$\begin{aligned}
 I(X;Y) &= H(Y) - H\left(\frac{X}{Y}\right) = H(X) - H\left(\frac{Y}{X}\right) \\
 &= H(X) + H(Y) - H(X,Y) \\
 &= \sum_{i=1}^{N_x} \sum_{j=1}^{N_y} P(X = x_i, Y = y_j) \log \frac{P(X = x_i, Y = y_j)}{P(X = x_i)P(Y = y_j)} \quad (14)
 \end{aligned}$$

Where  $H(X)$  and  $H(Y)$  are entropies of  $X$  and  $Y$  respectively;  $H(X/Y)$  and  $H(Y/X)$  are conditional entropies of  $X$  and  $Y$  respectively;  $H(X, Y)$  is joint entropy of  $X$  and  $Y$ ; and  $N_x, N_y$  are possible values of  $X$  and  $Y$  that it can take. The mutual information is always nonnegative, which is  $I(X; Y) \geq 0$ .<sup>[51]</sup> Since the mutual information of two data variable  $X$  and  $Y$  defined as above is not normalized;  $I(X; Y)$  can be quite small even if  $X$  and  $Y$  are highly correlated. Hence, the mutual information must be normalized by the maximal entropy of each of the contributing  $X$  and  $Y$ . The basic advantage of normalization is that it gives a high value for highly correlated data or pixel values in an image independent of the individual entropy. The normalized mutual information is defined as<sup>[30]</sup>:

$$\bar{I}(X;Y) = \frac{I(X;Y)}{\max\{H(X), H(Y)\}} \quad (15)$$

Here, we propose to use a threshold FCM clustering algorithm based on pairwise mutual information where a candidate cluster is formed by starting with the first image pixel and grouping the pixel that has smallest mutual-information-based distance with the centre of the cluster. The proposed mutual information based distance measure, used by FCM clustering discussed as above and described by Eqs.(10-14), is defined as:

$$d(X;Y) = 1 - \bar{I}(X;Y) = 1 - \frac{I(X;Y)}{\max\{H(X), H(Y)\}} \quad (16)$$

The working of the clustering approach is as follows: In each iteration, the pixel that has a minimal distance to the target pixel to the cluster is added. The process continues until the distance threshold is not crossed. A second candidate cluster is formed by starting with the second pixel and the same procedure is repeated. The pixels from the first candidate cluster are not removed from consideration and this process continues for all pixels. The largest candidate cluster is selected and retained. The pixels in the largest candidate cluster are removed from the whole image pixel set, and the entire procedure is repeated on the smaller pixel set. When the number of clusters reaches to a predefined cluster number, all the remaining pixels to the last cluster are added. The threshold may be chosen as the mean of the distances of all pixel pairs.

In this paper, the three classes of FCM clustering were used. These three classes include small, middle, and large. A switch-off cut-position (SWC) were used to select among the classes. The SWC having value zero and one gives cut between small and middle classes and cut between middle and large classes respectively. The threshold values for segmentation were calculated as follows:

```

If swc = 0//For cut between small and middle classes
Threshold level = {max[data (label = 1)]
                  + min[data (label = 2)]}/2;
else//swc = 1, For cut between middle and large classes
Threshold level = {max[data (label = 2)]
                  + min[data (label = 3)]}/2;
end
    
```

Where data in above expressions are one dimensional image data.

## Results and Performance Analysis

In this section, results and performance analysis of the proposed enhancement and segmentation techniques are

presented. For evaluation of the various mammogram segmentation approaches with the proposed one have been performed in terms of random index (RI), variation of information (VoI), and global consistency error (GCE). These performance measures are discussed as follows:

### Mammogram segmentation performance measures

#### Random index

The RI measure<sup>[52-53]</sup> was initially proposed for the evaluation of general clustering algorithms. The RI between test (S) and ground truth (G) is estimated by summing the number of pixel pairs with same label and number of pixel pairs having different labels in both S and G, and then dividing it by total number of pixel pairs. This gives a measure of similarity with value ranging from 0 when the two segmentations have no similarities (when one consists of a single cluster and the other consists only of clusters containing single points) to 1 when the segmentations are identical, that is when a higher value of RI close to 1 is preferred for perfect segmentation.

#### Variation of information

In this approach, the evaluation of segmentation algorithm is based on evaluating an affinity function that gives the probability of two pixels belonging to the same segment. The VoI or shared information distance is a measure of the distance between two clusters—partitions of elements.<sup>[54,55]</sup> If a clustering with clusters  $X_1, X_2, X_3, \dots, X_k$  is represented by a random variable with total number of clusters  $k = \{1, \dots, K\}$  such that  $P_i = \frac{|X_i|}{n}$ ,  $i \in X$  and  $n = \sum_k |X_i|$  then the variation of information (VoI) between two clusters and is defined as:<sup>[54-55]</sup>

$$\text{VoI}(X, Y) = H(X) + H(Y) - 2I(X, Y) \quad (17)$$

where  $H(X)$  and  $H(Y)$  are entropies of  $X$  and  $Y$ ; and  $I(X, Y)$  is mutual information between  $X$  and  $Y$ .  $\text{VoI}(X, Y)$  measures how much the cluster assignment for an item in cluster  $X$  reduces the uncertainty about the item's cluster in cluster  $Y$ . The value of  $\text{VoI}$  lies in between 0 and  $d$ , where  $d$  is the distance between clusters. Since it is a distance measure, hence a lower value of  $\text{VoI}$  close to zero indicates best segmentation.

#### Global consistency error

In papers<sup>[54,56]</sup> authors propose two metrics that can be used to evaluate the consistency of a pair of segmentations. These measures are designed in such a way that they are tolerant to refinement, i.e., if subsets of regions in one segmentation consistently merge into some region in the other segmentation the consistency error should be low. To compute the consistency error for a pair of images, at first a measure of the error at each pixel  $p_i$  is defined as follows:

$$E(S_1, S_2, p_i) = \frac{|R(S_1, p_i) \setminus R(S_2, p_i)|}{|R(S_1, p_i)|} \quad (18)$$

Where  $R(S_j, p_i)$  is the region in segmentation  $j$  that contains pixel  $p_i$ ,  $\setminus$  denotes set difference, and  $|\cdot|$  denotes set cardinality. This error measure evaluates to 0 if all the pixels in  $S_1$  are also contained in  $S_2$  thus achieving the tolerance to refinement discussed above. This measure is not symmetric, so for every pixel it must be computed twice, once in each direction. Given the error measures  $E$  at each pixel, the two segmentation error measures namely local consistency error (LCE) and GCE) defined by Martin *et al.*<sup>[54]</sup> reads

$$GCE(S_1, S_2) = \frac{1}{n} \min \left( \sum_i E(S_1, S_2, p_i), \sum_i E(S_2, S_1, p_i) \right) \quad (19)$$

and

$$LCE(S_1, S_2) = \frac{1}{n} \sum_i \min(E(S_1, S_2, p_i), E(S_2, S_1, p_i)) \quad (20)$$

Since  $LCE \leq GCE$ , hence GCE is a tougher measure than LCE and that's why it is used in this paper. A small value of GCE close to zero represents better segmentation. GCE quantify the amount of error in segmentation i.e., 0 signifies no error and 1 indicates no agreement.

## Results and Discussions

The proposed unsharp masking and crispening techniques were evaluated in terms of improvement in signal-to-noise ratio of the sample test mammographic images and its overall effect on the proposed segmentation method is also evaluated. The comparative study of the proposed combined enhancement and segmentation technique is presented with the other popular methods used for segmentation of mammographic images such as Otsu's thresholding, Texture based thresholding, k-means clustering, and FCM clustering based segmentation method based on Euclidian distance measure. For experimentation purposes, the 256 histogram bins were used in Otsu's gray level thresholding method. For k-means, fuzzy c-means, and the proposed segmentation method the initial number of clusters for the proposed FCM based segmentation method was set to three as it was associated with better performance. In texture based segmentation, an entropy based filter was used. For experimentation purposes, 25 test sample digital mammographic images were used. The average performance measures for the 10 sample images are shown in this paper; however the performance trend remained the same for other test images as well. The proposed segmentation approach was also tested on mammographic image analysis society (MIAS) database. Figure 2 shows the visual results of unsharp masking and crispening procedure in spatial domain. Table 2 and Figure 3 present results in terms

of signal-to-noise ratio (SNR) of original sample mammogram and improvement in SNR (ISNR) after applying proposed unsharp masking and crispensing method in wavelet domain. From Table 1 and Figure 3, it is observed that the proposed nonlinear complex diffusion (a partial differential equation based approach-PDE) based unsharp masking and crispensing methods is showing a good improvement over SNR values of the original mammogram which justifies that the proposed method is better capable of enhancing and highlighting the abnormalities in mammogram in details.

The first top row of Figure 4 shows visual results for initial steps before segmentation, in initial steps of the proposed method, the visual results of the original mammogram,

enhanced image by CLAHE method, unsharp masking and crispensing, and results after applying two levels of wavelet decomposition (bi-orthogonal) used in proposed method. During the 2D discrete wavelet decomposition (DWT) wavelet decomposition, a bi-orthogonal wavelet was used as a mother wavelet as it provides complete reconstruction of images.

The bottom row of Figure 4 shows the visual results for the various segmentation methods such as Otsu's thresholding, texture segmentation, k-means segmentation, Fuzzy S-means segmentation and the proposed segmentation method. From visual results, it is observed that the proposed segmentation approach is providing the better segmentation results in comparison to other methods and it is well capable

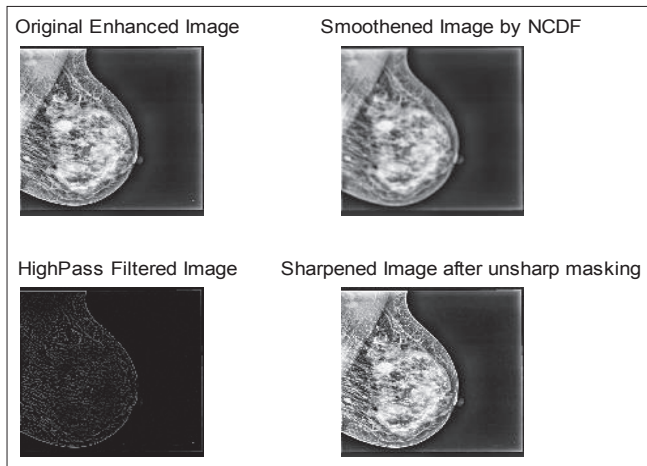


Figure 2: Visual results of unsharp masking and crispensing procedure in spatial domain

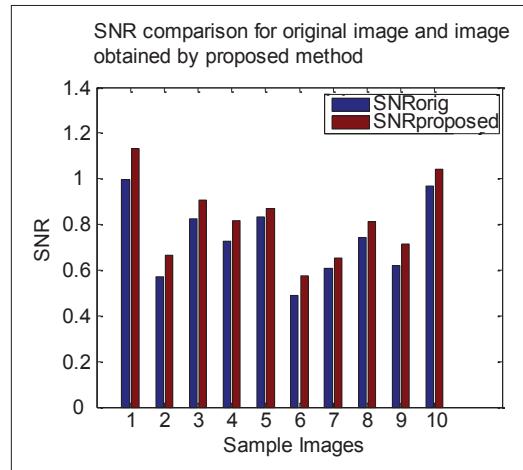


Figure 3: Comparison of SNR values of different mammograms for original image and image obtained after unsharp masking and crispensing

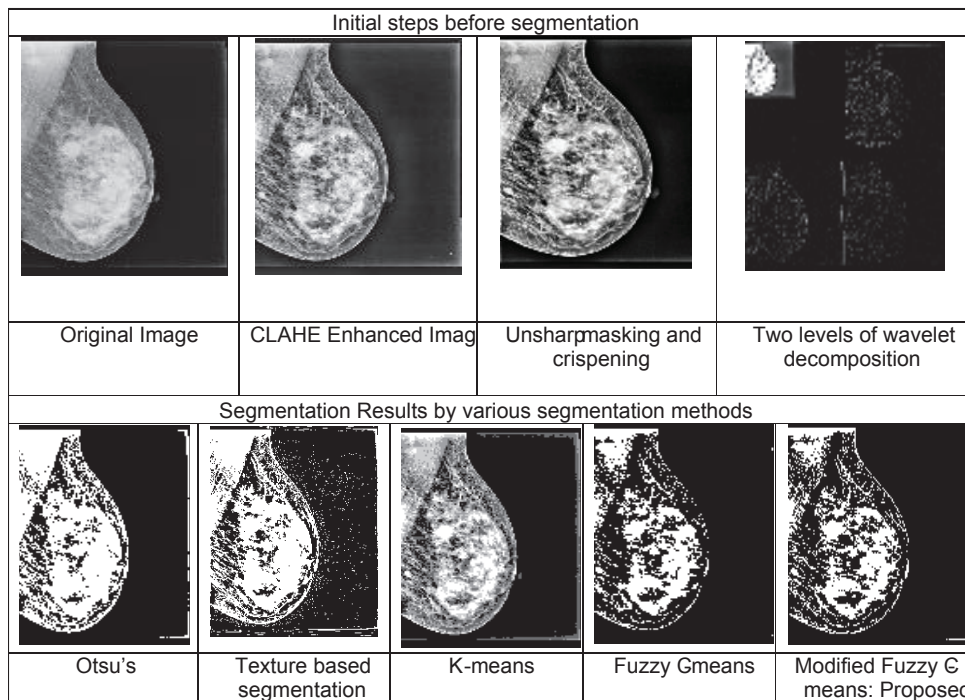


Figure 4: Visual results for (i) Initial steps before segmentation (ii) various segmentation methods and proposed one

of segmenting the all possible types of abnormalities such as tumours, micro-calcifications etc., that may be present in mammogram for breast cancer diagnosis.

Table 3 presents the evaluation of various segmentation methods and the proposed one in terms of RI, VoI, and GCE for 10 sample mammograms. The averaged values of RI, VoI, and GCE for 10 sample images are also shown which gives the average performance of the methods. For better segmentation results the value RI should be close to one and higher than the values related to other segmentation methods; and the values of VoI and GCE should be lower than that of the other segmentation methods.

Figure 5 shows comparison of RI values of various segmentation methods for 10 sample images. From Figure 5, it is observed that the values of RI for each sample image for the proposed method are higher than that of other methods signifying that the proposed method is performing better in comparison to other methods. Figure 6 shows comparison of average RI values of various segmentation methods for 10 sample images and the average RI value for proposed method is larger in comparison to other methods.

Figure 7 shows comparison of GCE of various segmentation methods for 10 sample images and Figure 8 shows comparison of average GCE values of various segmentation methods for 10 sample images. From Figures 7 and 8, it is observed that the GCE value of the proposed method is smaller than that of the other methods.

Figure 9 shows comparison of VoI values of various segmentation methods for 10 sample images and Figure 10 shows comparison of average VoI values of various segmentation methods for 10 sample images. From Figures 9 and 10, it is observed that the GCE value of the proposed method is smaller than that of the other methods.

**Table 2: Results in terms of signal-to-noise ratio of original sample mammogram and Improvement in SNR after applying proposed PDE based unsharp masking and crispensing method wavelet domain**

Sample mammographic image	SNR <sub>orig</sub> [dB]	SNR <sub>proposed</sub> [dB]
Image 1.jpg	0.9948	1.1308
Image 2.jpg	0.5719	0.6649
Image 3.jpg	0.8256	0.9050
Image 4.jpg	0.7280	0.8177
Image 5.jpg	0.8333	0.8696
Image 6.jpg	0.4909	0.5764
Image 7.jpg	0.6065	0.6513
Image 8.jpg	0.7433	0.8136
Image 9.jpg	0.6220	0.7153
Image 10.jpg	0.9670	1.0404

SNR: Signal-to-noise ratio, PDE: Partial differential equation

Table 4 shows comparison of execution time (in seconds) of various segmentation methods for sample image, image1.jpg of 2770 × 1770. Here, again it is observed that the proposed method is taking

**Table 3: Evaluation of segmentation methods in terms of RI, Vol, and GCE for 10 sample mammograms**

Segmentation method	Sample mammographic images	Performance measures		
		Rand index (higher better)	GCE (lower better)	Variation of Information (lower better)
Otsu's segmentation	Image 1	0.4912	0.0996	6.0428
	Image 2	0.6418	0.028	2.3573
	Image 3	0.6213	0.0457	3.2674
	Image 4	0.6355	0.0531	3.7942
	Image 5	0.512	0.063	3.6347
	Image 6	0.5952	0.0631	4.1359
	Image 7	0.5835	0.0889	4.5199
	Image 8	0.5819	0.0489	3.6309
	Image 9	0.6502	0.0432	3.4294
	Image 10	0.5649	0.0305	3.9478
	Average values for 10 images	0.58775	0.0564	3.87603
Texture based	Image 1	0.4914	0.1486	6.308
	Image 2	0.5631	0.075	2.6206
	Image 3	0.5677	0.0687	3.4205
	Image 4	0.5007	0.1078	4.0988
	Image 5	0.5866	0.1174	3.9355
	Image 6	0.5799	0.1105	4.4188
	Image 7	0.4671	0.142	4.8293
	Image 8	0.4761	0.1018	3.9233
	Image 9	0.6287	0.1096	3.7849
	Image 10	0.6418	0.0872	4.2642
	Average values for 10 images	0.55031	0.10686	4.16039
K-means	Image 1	0.6931	0.2776	6.0135
	Image 2	0.703	0.0858	2.1235
	Image 3	0.7376	0.2172	3.3187
	Image 4	0.7137	0.2903	3.9285
	Image 5	0.496	0.1056	3.5329
	Image 6	0.5775	0.1125	3.0592
	Image 7	0.3784	0.1275	4.3427
	Image 8	0.4476	0.0868	3.4887
	Image 9	0.4433	0.0729	3.4829
	Image 10	0.5982	0.1019	3.0089
	Average values for 10 images	0.57884	0.14781	3.62995
Fuzzy C-means	Image 1	0.6563	0.1193	6.3086
	Image 2	0.7495	0.0254	2.4965
	Image 3	0.6419	0.0538	3.4991
	Image 4	0.7001	0.0759	4.0550
	Image 5	0.5755	0.0714	3.8951
	Image 6	0.6218	0.0684	4.4564
	Image 7	0.5773	0.0803	4.7630
	Image 8	0.5634	0.0504	3.8473
	Image 9	0.5323	0.0492	3.6641
	Image 10	0.631	0.0865	4.4152
	Average values for 10 images	0.62491	0.06806	4.14004

Contd...

**Table 3: Continued**

Segmentation method	Sample mammographic images	Performance measures		
		Rand index (higher better)	GCE (lower better)	Variation of Information (lower better)
Proposed modified segmentation Method in wavelet domain	Image 1	0.7467	0.0302	3.9882
	Image 2	0.7963	0.0101	2.4465
	Image 3	0.7157	0.0211	2.6903
	Image 4	0.7966	0.02	2.9275
	Image 5	0.6397	0.021	2.9288
	Image 6	0.6576	0.0112	3.2108
	Image 7	0.6093	0.0312	3.6474
	Image 8	0.6448	0.004	3.5804
	Image 9	0.6845	0.0101	3.9357
	Image 10	0.8314	0.0023	2.7724
Average values for 10 images		0.71226	0.01612	3.2128

6.561 seconds whereas the traditional FCM method is taking 148.94 seconds.

Therefore, from the results obtained it is observed that the proposed segmentation method is performing better in comparison to all other methods in consideration and it is well capable of segmenting the abnormalities in mammograms.

**Conclusions**

In this paper, a nonlinear complex diffusion based unsharp masking and crispening method was proposed for enhancement of abnormalities found in mammograms for the breast cancer detection. Further, a modified FCM segmentation method was proposed in wavelet domain. The distance measure for clustering purposes, in the proposed segmentation method, was based on the mutual information of image pixels. Two levels of (DWT) was

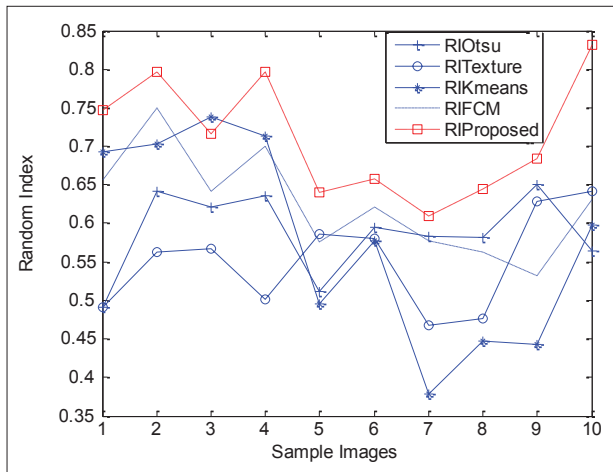


**Figure 5: Comparison of random index values of various segmentation methods for 10 sample images**

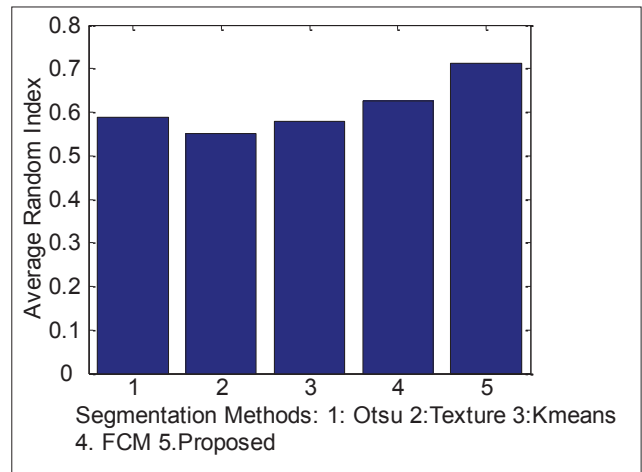


**Figure 6: Comparison of average random index values of various segmentation methods for 10 sample images**

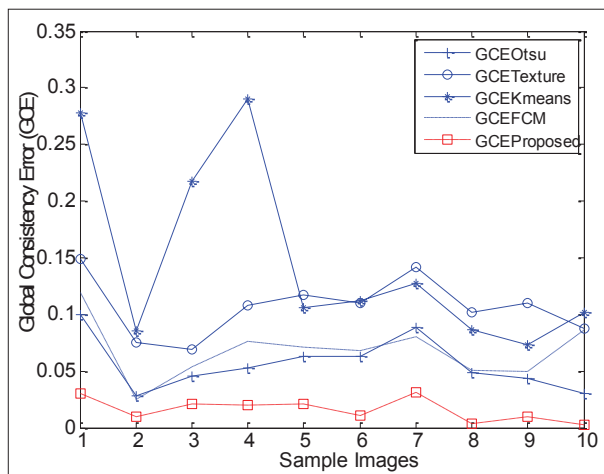


**Figure 7: Comparison of global consistency errors of various segmentation methods for 10 sample images**

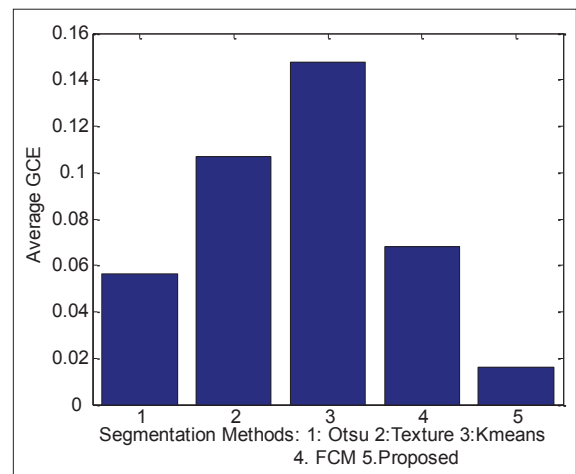


**Figure 8: Comparison of average GCE values of various segmentation methods for 10 sample images**

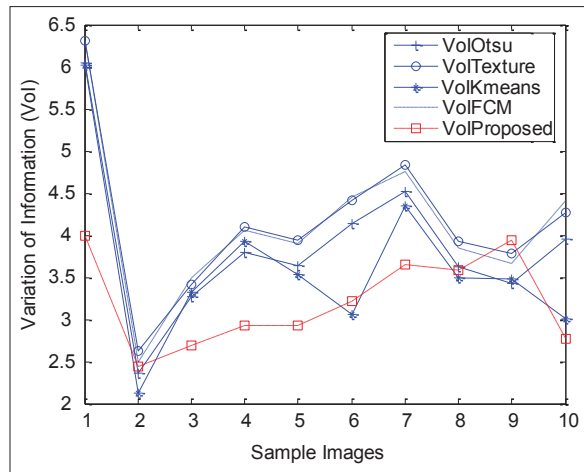


Figure 9: Comparison of variation of information values of various segmentation methods for 10 sample images

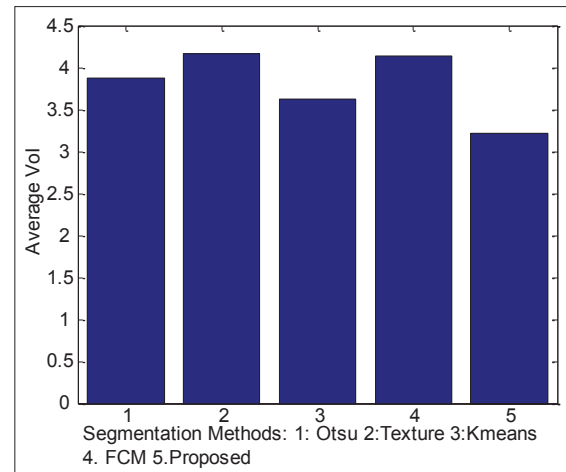


Figure 10: Comparison of average Vol values of various segmentation methods for 10 sample images

**Table 4: Comparison of execution time (in seconds) of various segmentation methods for 10 sample images**

Segmentation method	Execution time in seconds
Otsu's thresholding <sup>[34-35]</sup>	0.205195
Texture based segmentation <sup>[36]</sup>	34.21528
K-means <sup>[31]</sup>	18.17642
Fuzzy C-means <sup>[38]</sup>	148.9427
Proposed	6.561793

used for image decomposition and transformation. The mother wavelet used for the wavelet decomposition was bi-orthogonal wavelets as it provides full reconstruction of images. For experimentation purposes, the initial number of clusters for the k-means, fuzzy c-means, and the proposed segmentation method was set to three as it was associated with better performance. The performance of the proposed enhancement method was evaluated in terms of signal-to-noise ratio (SNR). The performance of the proposed segmentation method was evaluated in terms of three measures such as RI (RI), GCE, and Vol. The performance of the proposed method and other segmentation methods in consideration were evaluated both qualitatively and quantitatively. The execution time of the proposed method was also lower in comparison to its best counterpart which was FCM with Euclidian distance. The comparisons of the performances of the proposed method with the other segmentation methods were also presented in the paper. Therefore, from the obtained results, it can be concluded that the proposed enhancement and segmentation framework is computationally cheaper, producing better results in comparison to other methods, alleviate the problems related to the Euclidian distance measure in traditional FCM based segmentation and reduces the false positives and outliers during the segmentation of the mammograms. Hence, the proposed method may be

a better choice for segmentation of mammograms for the breast cancer detection.

## References

1. Available from: <http://www.cancer.org/Cancer/BreastCancer/DetailedGuide/breast-cancer-keystatistics> [Last accessed on 2013 Oct 14].
2. Lai SM, Li X, Biscof WF. On techniques for detecting circumscribed masses in mammograms. *IEEE Trans Med Imaging* 1989;8:377-86.
3. Cheng HD, Shi XJ, Min R, Hu LM, Cai XP, Du HN. Approaches for automated detection and classification of masses in mammograms. *Pattern Recogn* 2006;39:646-68.
4. Ganesan K, Acharya UR, Chua CK, Min LC, Abraham KT, Ng KH. Computer-aided breast cancer detection using mammograms: A review. *IEEE Rev Biomed Eng* 2013;6:77-98.
5. Tang, J, Rangayyan RM, Xu J, El Naqa I, Yang Y. Computer-aided detection and diagnosis of breast cancer with mammography: Recent advances. *IEEE Trans Inf Technol Biomed* 2009;13:236-51.
6. Rangayyan RM, Ayres FJ, Desautels JE. A review of computer-aided diagnosis of breast cancer: Toward the detection of subtle signs. *J Franklin Inst* 2007;312-48.
7. Nam SH, Choi JY. A method of image enhancement and fractal dimension for detection of microcalcifications in mammogram. In: *Proceedings of the 20<sup>th</sup> Annual International Conference of the IEEE Engineering in Medicine and Biology Society, Hong Kong. Vol. 2. 1998. p. 1009-12.*
8. Wilson M, Hargrave R, Mitra S, Shieh YY, Roberson GH. Automated detection of microcalcifications in mammograms through application of image pixel remapping and statistical filter. In: *Proceedings of the IEEE Symposium on Computer-based Medical Systems, Lubbock, TX, USA; 1998. p. 270-4.*
9. Wongsritong K, Kittayarasirawat K, Cheevasuvit F, Dejhan K, Sombonkaew A. Contrast enhancement using multipole histogram equalization with brightness preserving, in proceedings: *IEEE Asia-Pacific Conference on Circuits and Systems, Chiangmai. 1998. p. 455-8.*
10. Cheng HD, Shi XJ. A simple and effective histogram equalization approach to image enhancement. *Dig Sig Proc* 2004;14:158-70.
11. Pisano ED, Zong S, Hemminger BM, DeLuca M, Johnston RE, Muller K, et al. Contrast limited adaptive histogram equalization image processing to improve the detection of simulated spiculations in dense mammograms. *J Digit Imaging* 1998;11:193-200.
12. Xiong Y, Lam CF, Frey GD, Croley MR. Contrast enhancement of

- mammogram by image processing. In proc.: *SPIE 1898, Medical Imaging 1993: Image Processing*, 8, Newport Beach, CA; 1993. p. 852-8.
13. Dhawan AP, Le Royer E. Mammographic feature enhancement by computerized image processing. *Comput Methods Programs Biomed* 1988;27:23-35.
  14. Urias JF. Feature enhancement of images using maximal contrast pixel to pixel. *Appl Opt* 1991;30:4598-9.
  15. Qian W, Clarke LP, Kallergi M, Clark RA. Tree-structured nonlinear filters in digital mammography. *IEEE Trans Med Imaging* 1994;13:25-36.
  16. Chang CM, Laine A. Enhancement of mammograms from oriented information. In: *IEEE International Conference on Image Processing*, Santa Barbara, CA 1997. vol. 3, p. 524-7.
  17. Mallat S, Zhong S. Characterization of signals from multiscale edges. *IEEE Trans Pattern Anal Mach Intell* 1992;14:710-32.
  18. Lu J, Healy DM, Weaver JB. Contrast enhancement of medical images using multiscale edge representation. *Opt Eng* 1994;33:2151-61.
  19. Laine A, Fan J, Yang W. Wavelets for contrast enhancement of digital mammography. *IEEE Eng Med Biol* 1995;14:536-50.
  20. Laine AF, Schuler S, Fan J, Huda W. Mammographic feature enhancement by multiscale analysis. *IEEE Trans Med Imaging* 1994;13:725-40.
  21. Petrick N, Chan HP, Sahiner B, Wei D. An adaptive density weighted contrast enhancement filter for mammographic breast mass detection. *IEEE Trans Med Imaging* 1996;15:59-67.
  22. Tsirikolias K, Mertzios BC. Edge extraction and enhancement using coordinate logic filters. *Image Process. Theory Appl* 1993;251-4.
  23. Rocha A, Tong F, Yan ZZ. Logic filter for tumor detection on mammograms. *J Comput Sci Technol* 2000;15:629-32.
  24. Kobatake H, Yoshinaga Y. Detection of spicules on mammogram based on skeleton analysis. *IEEE Trans Med Imaging* 1996;15:235-45.
  25. Kobatake H, Murakami M, Takeo H, Nawano S. Computerized detection of malignant tumors on digital mammograms. *IEEE Trans Med Imaging* 1999;18:369-78.
  26. Polakowski WE, Cournoyer DA, Rogers SK, DeSimio MP, Ruck DW, Hoffmeister JW, *et al.* Computer-aided breast cancer detection and diagnosis of masses using difference of gaussians and derivative-based feature saliency. *IEEE Trans Med Imaging* 1997;16:811-9.
  27. Gonzalez RC. *Digital image processing*. India: Prentice Hall; 2<sup>nd</sup> Edition, 2003.
  28. Oliver A, Freixenet J, Marti J, Perez E, Pont J, Denton ER, *et al.* A review of automatic mass detection and segmentation in mammographic images. *Med Image Anal* 2010;14:87-110.
  29. Srivastava S, Sharma N, Singh SK. "Image analysis and understanding techniques for breast cancer detection from digital mammograms in research developments" in: Srivastava, R., Singh, SK, Shukla, KK (editors). *Computer Vision and Image Processing: Methodologies and Applications*. IGI Global, USA; 2013. Ch. 8 p. 123-8.
  30. Zhou X, Wang X, Dougherty ER, Russ D, Suh E. Gene clustering based on clusterwise mutual information. *J Comput Biol* 2004;11:147-61.
  31. Sridhar S. *Digital image processing*. India: Oxford University Press First Edition; 2011.
  32. Srivastava S, Sharma N, Singh SK, Srivastava R. Analysis of image segmentation techniques in the design of a CAD tool for early breast cancer detection from mammograms. In proc: *International Conference on Artificial Intelligence and Soft Computing (AISC-2012)*, 7-9 December 2012, IIT-BHU, Varanasi, India, p. 65-71.
  33. Dogra DP, Majumdar AK, Sural S. Evaluation of segmentation techniques using region area and boundary matching information. *J Vis Commun Image Represent* January 2012;23, Issue 1;150-60.
  34. Otsu N. A threshold selection method from gray-level histogram. *IEEE Trans Sys Man Cyber* 1979;9:62-6.
  35. Sezgin M, Sankur B. Survey over image thresholding techniques and quantitative performance evaluation. *J Electron Imaging* 2004;13:146-65.
  36. Karahaliou A, Skiadopoulos S, Boniatis I, Saketllaropoulos P, Likaki E, Panayiotakis G, *et al.* Texture analysis of tissue surrounding microcalcifications on mammograms for breastcancer diagnosis. *Br J Radiol* 2007;80:648-56.
  37. Cai W, Chen S, Zhang D. Fast and robust fuzzy c-means clustering algorithm incorporating local information for image segmentation. *Pattern Recogn* 2007;40:825-38.
  38. Bezdek JC, Ehrlich, R, Full, W., FCM: The Fuzzy c-means clustering algorithm, *Computers and Geosciences*, Vol. 10, NO. 2-3, p. 191-203, 1984.
  39. Srivastava R, Gupta JR, Parthasarthy H, Srivastava S. PDE based unsharp masking, crispening and high boost filtering of digital images. In: Ranka S, Aluru S, Buyya R, Chung Y.-C., Dua S, Grama A, *et al.* editors. *Contemporary Computing, Part-I, Communications in Computer and Information Science (CCIS)*. Vol. 40. Germany: Springer Berlin Heidelberg; 2009. p. 8-13.
  40. Perona P, Malik J. Scale space and edge detection using anisotropic diffusion. *IEEE Transactions on Pattern Analysis and Machine Intelligence*. Vol. 12, Issue 7 1990. p. 629-39.
  41. Gilboa G, Sochen N, Zeevi YY. Image enhancement and denoising by complex diffusion processes. *IEEE Trans Pattern Anal Mach Intell* 2004;25:1020-36.
  42. Press HW, Teukolsky A, Vetterling ST, Flannery PB. *Numerical Recipes in C: The Art of Scientific Computing*. 2<sup>nd</sup> ed.. Cambridge University Press, USA; 1992. pp. 827-844
  43. Chen S, Zhang D. Robust image segmentation using FCM with spatial constraints based on new kernel-induced distance measure. *IEEE Trans Syst Man Cybern B Cybern* 2004;34:1907-16.
  44. Hathaway RJ, Bezdek JC. Generalized fuzzy c-means clustering strategies using Lp norm distance. *IEEE Trans Fuzzy Syst* 2000;8:576-582.
  45. Jajuga K. L1 norm based fuzzy clustering. *Fuzzy Sets Syst* 1991;39:43-50.
  46. Leski J. An "insensitive approach to fuzzy clustering. *Int J Appl Math Comp Sci* 2001;11:993-1007.
  47. Pham DL, Prince JL. An adaptive fuzzy C-means algorithm for image segmentation in the presence of intensity in homogeneities. *Pattern Recogn Lett* 1999;20:57-68.
  48. Tolias YA, Panas SM. On applying spatial constraints in fuzzy image clustering using a fuzzy rule-based system. *IEEE Signal Proc Lett* 1998;5:245-7.
  49. Liew AW, Leung SH, Lau WH. Fuzzy image clustering incorporating spatial continuity. *Inst Elec Eng Vis Image Signal Proc* 2000;147:185-92.
  50. Pham DL. Fuzzy clustering with spatial constraints. In: *IEEE Proc Int Conf Image Processing*, New York; 2002. vol. 2, p. II-65-II.
  51. Rand W. Objective criteria for the evaluation of clustering methods. *J Acoust Soc Am* 1971;66:846-85.
  52. Unnikrishnan R, Pantofaru C, Hebert M. Toward objective evaluation of image segmentation algorithms. *IEEE Trans Pattern Anal Mach Intell* 2007;29:929-44.
  53. Martin D. An empirical approach to grouping and segmentation. PhD dissertation, Univ. of California, Berkeley; Report No. UCB/CSD-3-1268. August 2003. Computer Science Division (EECS).
  54. Fowlkes C, Martin D, Malik J. Learning affinity functions for image segmentation. *Proc IEEE Conf Comput Vision Pattern Recogn* 2003;2:54-61.
  55. Martin D, Fowlkes C, Tal D, Malik J. A database of human segmented natural images and its application to evaluating segmentation algorithms and measuring ecological statistics. *Proc International Conference on Computer Vision ICCV 2001*;2:416-25.
  56. Mohabey, Ray AK. Fusion of rough set theoretic approximations and FCM for color image segmentation. *IEEE Int Conf Syst Man Cybernet* 2000;2:1529-34.
  57. Boss RS, Thangavel K, Daniel DA. Mammogram image segmentation using rough clustering. *Int J Res Eng Technol* 2013;66-77.
  58. Hassanien AE, Abraham A, Peters JF, Schaefer G, Henry C. Rough sets and near sets in medical imaging: A review. *IEEE Trans Inf Technol Biomed* 2009;13:955-68.
  59. Castillejos H, Volodymyr P. Fuzzy image segmentation algorithms

in wavelet domain, fuzzy logic – algorithms, techniques and implementations. Chapter 7, pp. 127-146 In: Dadios E, editor. 28 March 2012. Available from: [Http://www.intechopen.com/books/fuzzy-logic-algorithms-techniques-and-implementations/fuzzy-image-segmentation-algorithms-in-wavelet-domain](http://www.intechopen.com/books/fuzzy-logic-algorithms-techniques-and-implementations/fuzzy-image-segmentation-algorithms-in-wavelet-domain) [Accessed online on 2013 Nov 06].

**How to cite this article:** Srivastava S, Sharma N, Singh SK, Srivastava R. A combined approach for the enhancement and segmentation of mammograms using modified fuzzy C-means method in wavelet domain. *J Med Phys* 2014;39:169-83.

**Source of Support:** Nil, **Conflict of Interest:** None declared.